Scanning Microscopy

Volume 5 | Number 1 Article 3

10-12-1990

A Loading Device for Fracture Testing of Compact Tension Specimens in the Scanning Electron Microscope

Jügen Rödel
Lehigh University

James F. Kelly
National Institute of Standards and Technology

Mark R. Stoudt
National Institute of Standards and Technology

Stephen J. Bennison
Lehigh University

Scanning Microscopy, Vol. 5, No. 1, 1991 (Pages 29-35)
Scanning Microscopy International, Chicago (AMF O'Hare), IL 60666 USA

0891-7035/91$3.00+.00

A LOADING DEVICE FOR FRACTURE TESTING OF COMPACT TENSION SPECIMENS IN THE SCANNING ELECTRON MICROSCOPE

Jürgen Rödel[1], James F. Kelly*, Mark R. Stoudt and Stephen J. Bennison[1]

Ceramics Division
National Institute of Standards and Technology
Gaithersburg, MD 20899

1. Guest Scientist on leave from the Department of Materials Science and Engineering, Lehigh University, Bethlehem, PA 18015.

(Received for publication May 26, 1990, and in revised form October 12, 1990)

Abstract

A loading device for performing fracture experiments on compact tension specimens in the SEM has been designed. Its key elements are a piezoelectric translator for applying controlled displacements to the loading points on the specimen and a load cell to measure applied loads. The effective transmission of displacement from the piezoelectric driver to the specimen was found to be the major mechanical design problem. The peripheral equipment includes a function generator and a high voltage amplifier that drives the piezoelectric translator as well as a video overlay and standard video equipment to record the image continuously during the course of the experiment. A case study on alumina describes qualitative observations on the toughening mechanism, crack-interface bridging, operating in this material. Quantitative information pertaining to the closure stresses associated with this toughening mode can be obtained by measuring the crack profile.

KEY WORDS: Scanning electron microscopy, cracks, crack profile, in-situ, fracture toughness, microstructure, alumina

*Address for correspondence:
James F. Kelly,
National Institute of Standards and Technology
Bldg. 223, Rm. A256
Gaithersburg, MD 20899
Phone No. (301) 975-5794

Introduction

The science of fractography, viz, the postmortem observation of features associated with fracture, is an important element of any investigation into mechanical behavior of materials [12]. Fractography embodies a variety of techniques which can provide invaluable insights into fracture modes, loading histories and the role of microstructure in failure for a range of different materials.

The postmortem nature of fractography, however, ultimately places a restriction on its utility. Events influencing fracture which leave no visible traces after specimen failure go undetected. A case in point is the phenomenon of crack-interface bridging which is responsible for rising crack resistance (R-curve) behavior in many monolithic ceramics such as aluminum oxide [9,11,15,16]. In this mechanism, intact grains well behind the primary crack tip bridge the crack walls, shield it from the applied stress intensity field (K_a) and lead to increased crack resistance (toughness) with crack extension; after failure the bridges have been destroyed. Identification of grain bridging has only been attained through careful in situ studies of crack growth using optical microscopy [16]. Recognition that the toughness behavior of many ceramic systems may be determined by grain bridging and other wake-associated mechanisms [6] has highlighted the importance of in situ observations of fracture events.

The aim of the present work is to develop a fixture for in situ testing of materials in the scanning electron microscope (SEM). The superior resolution afforded by the SEM provides two significant advantages over existing optically based systems. First, greater detail of crack - microstructure interactions, such as grain bridging, can be obtained. Such information is critical to the development of models describing the toughening and R-curve properties of ceramics [4]. Second, quantitative information on the stress intensity fields (K-fields) can be gained from direct measurements of crack profiles. In the case of ceramics, crack opening displacements typically range from 0 μm (at the crack tip) to 1-2 μm (at the crack mouth) and, as such, cannot be readily

measured by optical techniques.

A number of SEM-based testing systems have been described before, designed for tensile loading of test bars [5], four-point bending [8], double torsion [17] and wedge-loaded DCB-type specimen [19]. Special requirements, in particular the ability to measure the propagation and the profile of long cracks, necessitated the development of a loading stage for compact tension specimens. Profile measurements of long cracks in particular, allow a calculation of the stress-separation function [14], which is the key material characteristic determining R-curve behavior [4].

In this paper a design for such an SEM-based testing system is presented. Mechanical, electrical and imaging requirements are described, and results from a case study of crack growth in aluminum oxide are detailed to demonstrate the capabilities of the loading stage.

Instrument Design

The fracture device was designed for use in an AMRAY [1] SEM [2]. This particular instrument offers the advantage of a large specimen chamber (more than 30 cm in each dimension) and allows easy access to the SEM stage which is connected to the door and therefore swings out when the chamber is opened.

For this case study tests were run at 20 kV accelerating voltage with the sample surface perpendicular to the beam.

Mechanical Considerations

The specimen geometry of choice is compact tension (round or rectangular) according to the ASTM E 399 specification [1]. This geometry was chosen for several reasons. First, the stress intensity solutions for the applied stress field (K_a) are available. Second, for materials, like alumina, which experience closure forces due to crack-interface bridging in the crack wake [15,16], the additional requirement, that the crack be long compared to the bridging zone, can be satisfied with this geometry. Then K_a values can readily be calculated from measurements of the applied load and crack length. Third, the crack path is stable [2] (shows no deviation from a straight line). Fourth, disk-shaped specimens are readily prepared using conventional ceramics processing.

Figure 1 shows schematically the loading stage and Figure 2 is a photograph of the fixture. The heart of the device is a piezoelectric translator (T) [3] (see also [8]) capable of displacements up to 85 μm and maximum force of 1,000 N when a voltage of 1 kV is applied. The force is transmitted to the specimen via a system of two pivot arms (P) and two loading arms (L). The pivot arms rotate on pivot points (PP) which are rigidly attached to a rectangular baseplate. The loading arms

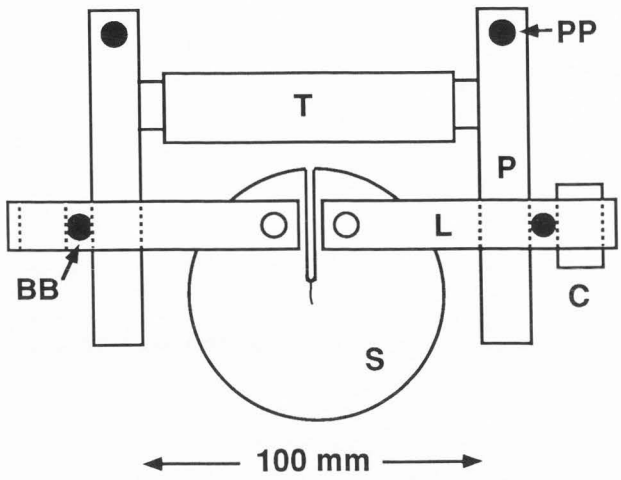

Figure 1. Schematic of device for in situ SEM observations of compact tension specimen. T = piezoelectric translator, C = load cell, P = pivot arms, L = loading arms, PP = pivot point, BB = ball bearing and S = specimen.

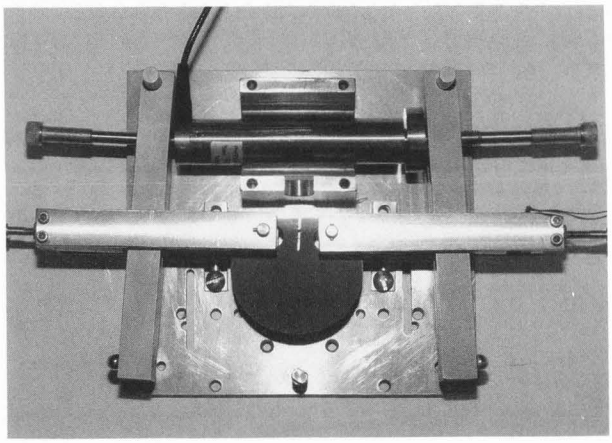

Figure 2. Photograph of the loading device containing disc compact tension specimen.

[1] AMRAY 1830, Amray Inc., Bedford, MA.

[2] Certain commercial equipment are identified in this paper in order to adequately specify the experimental procedure. Such identification does not imply recommendation or endorsement by the NIST, nor does it imply that the equipment identified is necessarily the best available for the purpose.

[3] PI Model P-245.50, Physik Instrumente, D7571 Waldbronn, FRG.

connect to the pivot arms via two ball bearings (BB) which allow rotational alignment of the system and prevent the application of bending moments to the specimen. A strain gauge load cell [4] is placed in one loading arm and allows monitoring of the applied load between 0 and 2,300 N.

The primary mechanical design requirement is the efficient transmission of displacement from the piezoelectric translator to the specimen. Losses in displacement due to the compliance of the loading train are minimized by constructing the elements from (non-magnetic) stainless steel and fabricating the pivot points to tolerances of ~25 μm. Despite these precautions displacement losses were considerable in our early designs. The final arrangement, presented in Figure 1, places the piezoelectric translator between the pivot points (PP) and the load application points (BB) to the loading arm (L). At first glance this may appear to give a poor mechanical advantage, with the force applied through the piezoelectric translator being reduced to 40% at the loading arms. However, the design ensures that sufficient displacement is available at the crack mouth to drive cracks in ceramics of this specimen geometry. Specimens are also routinely prestressed with two screws, which link the piezoelectric translator to the pivot arms, before placing the loading device into the SEM chamber. The load transmission characteristics result in mechanical testing effectively in a constant load mode [2] due to the stored elastic energy in the loading train.

If the loading stage is used for cyclic loading applications, a slight specimen shift is noticeable. This displacement was less than 6 μm.

Electrical Considerations

The supply voltage for the piezoelectric translator, and the supply and signal voltages for the load cell (5V power supply and standard voltmeter) are connected into the specimen chamber via three electrically isolated BNC type feedthroughs mounted on a side port of the SEM. The piezoelectric translator is driven by a high voltage amplifier [5] which, when fed with a function generator, affords application of controlled (e.g. cyclic) loading. The relatively large capacitance (113 nF) of the translator in combination with the low current output of the power supply (1.8 mA) places an upper bound on the range of available frequencies (≈2 Hz).

Imaging requirements

The physical characteristics of the compact tension test fixture along with the requirement for real time imaging act to limit the image resolution in three ways: increased working distance, reduced vibrational stability, and higher specimen current. The piezoelectric driver and raised pivot rods require operating at a working distance of 30 mm to avoid contacting the secondary electron detector and the final lens. Since the best resolution obtained on this microscope is 5 nm at the minimum working distance of 5 mm, this increase in working distance alone decreases the secondary image resolution by a factor of about six. Additionally, the requisite stiffness for transmitting the load from the driver, through the loading and pivot arms, to the test specimen with minimal flexure of the arms, necessitates a large mass of nearly two kilograms which must be supported by the SEM stage. This increased load on the stage, together with the requirement that the test specimen be minimally constrained, significantly increases the vibrational sensitivity of the system. An improvement of the fixture support has been achieved by bolting the fixture to the SEM stage in addition to having the standard pin support. The third factor influencing the electron spot size is the beam current. A compromise between resolution and the ability to follow crack propagation in real time resulted in the use of a 200 μm final aperture with the condenser lens adjusted to give a beam current of 100 pA. The combination of these operating conditions limits the resolution of the secondary image to approximately 70 nm.

Prior to full crack formation, highly polished, gold-coated specimen surfaces provide little contrast for secondary electron imaging. The charging of newly exposed non-coated material subsequent to crack extension, however, provides a readily detectable secondary electron signal. For more complex microstructures, backscattered electron imaging has proven useful in identifying the crack path relative to specific microstructural phases or grain boundaries. However, the relatively slow response time of the solid state backscatter electron detector, requiring scan times of at least 30 s/frame make this mode impractical for live time monitoring of crack propagation.

The rapid scan mode of the AMRAY Model 1830 SEM operates at a scan rate of 5 frames/s. The selected signal is processed through an integral 512 by 512 pixel frame buffer which displays the image at a standard TV rate of 30 frames/s. This capability for continuous display at TV rate enables the direct recording of the secondary image using a video cassette recorder (VCR). The SEM image is superimposed with the load cell output voltage using a video text overlay [6]. Photographic recording via instant film can also be done, either directly from the frame buffer, or by bypassing the buffer to obtain an increased line density in the recorded image.

---

[4] Sensotech, LFH-71, Sensotech, Columbus, OH 43212.

[5] PI Model P-263, Physik Instrumente, D7517 Waldbronn, FRG.

[6] VT0232 Video Text Overlay, Linkam Scientific Instruments Ltd., Tadworth, UK.

Case Study

We proceed to illustrate the capabilities of the fracture device by discussing some results from a case study on crack propagation in alumina.

An alumina disk, 4 mm thick and with a diameter of 100 mm, was prepared by hot pressing alumina powder [7] for 3 hours at 1650°C under a uniaxial pressure of 35 MPa. The pressed slab was found to be pore-free with an average grain size of 11 μm. It was then ground to 1 mm thickness and polished with diamond pastes of grade 15 μm down to 1 μm. A compact tension specimen was machined by drilling holes for the loading arms and cutting a notch. The stability of the sample with respect to crack propagation was enhanced by extending the notch at an angle of 28° to the specimen surface, which gave the geometry of a quasi-chevron notch, with the notch being extended about 2 mm on the unpolished (lower) surface. A Vickers hardness indention (P = 50 N) was placed about 200 μm in front of the notch on the polished surface. The radial cracks emanating from the elastic-plastic zone in the direction of the notch were then extended under tension with the loading device placed on an optical microscope. Subsequently, the indented region was cut out to leave a precrack of about 100 μm length. After the first crack propagation run (for $\simeq$ 2mm) the specimen was removed and resawn again, for second and third runs. Etching to reveal the microstructure of the specimen was purposely avoided, since cracks following a grain boundary groove are difficult to detect in the crack tip region.

Crack propagation under applied tensile loading in the SEM was found to be stable in the quasi-chevron region. The load was increased until crack extension occurred (typically for 10 - 50 μm) and the crack arrested again. The required loading increments for crack instability to occur were found to be between 5 and 15 N with the total applied loading in the range between 200 and 300 N.

Microscopical observations during crack extension are classified here into two categories: events at the crack tip and events in the crack wake. In the first category, the mode of crack propagation, discontinuous in nature, in contrast to slow crack growth in glass in high vacuum [18], can be monitored. The occurrence of subsidiary cracking - either secondary cracking or microcracking in a zone [7] - can also be followed while the crack passes through a given region in the material. Microcracking in particular has been a focal point of recent considerations and has been invoked as one of the possible toughening mechanisms in ceramics [6]. The R-curve in alumina, in particular, was originally attributed to this mechanism [13]. With the resolution now available using the loading device in the SEM, the creation of microcracks (of lengths down to at least one grain facet and openings down to about 50 nm) can be detected. No such microcracking was observed in the particular alumina studied in this case.

Observations of the crack wake focus on bridge evolution [14]. A bridge is here defined as any microstructural element connecting the crack faces which gives rise to a closure force. An example is given in Fig. 3 a,b with a closure force across the crack surfaces being applied at A. This force causes the secondary crack at location B to open. With further crack propagation the opening of the primary crack increases, the closure force diminishes and the secondary crack at B closes (Fig. 3b). Note also the creation of a new secondary crack at position C in Fig. 3b. Observations such as the one described help understand the origin of closure forces in the crack wake. The crack opening displacement of secondary cracks as a function of the opening of the primary crack can be utilized to measure the relative closure stress at given regions while the crack propagates through the material [14].

The existence of closure forces in the crack wake can further be demonstrated and, in fact, numerically evaluated by measuring the crack opening (COD) as a function of distance from the crack tip [3].

Crack opening displacements are measured by imaging cracks at a magnification of 30, 000, taping the image and, after the experiment, measuring the opening from the video monitor. In ceramics we are typically concerned with crack opening displacements in the range of 50 to 2000 nm. Since standard optical techniques are not able to provide this type of resolution, SEM techniques are required. An accuracy of about 70 nm is currently obtained, although relative measurements can be made to 30 nm precision.

An example of three such measurements is given in Fig. 4 for the alumina studied. The profile is found to be linear in first approximation, which is in contrast to the parabolic profile of cracks with stress-free surfaces [10]. Closure forces arising from discrete bridges are commonly combined in a continuum description to give a continuous closure stress acting on the crack faces. This closure stress can be given as a function of distance from the crack tip [3], and, more fundamentally, as a function of the local crack opening displacement. If this description is used, the experimentally obtained profile can be related through an integral equation [14] to the closure force as a function of distance from the crack tip.

An additional route to obtaining quantitative information on the micromechanics of microstructural elements in the crack wake is given by recording crack opening displacements during loading/unloading. These measurements give further insight about the nature of the closure forces (frictional, elastic). In the

---

[7] Sumitomo AKP-HP grade (99.995% pure, 0.5μm crystallites), Sumitomo Chemical America, New York, NY.

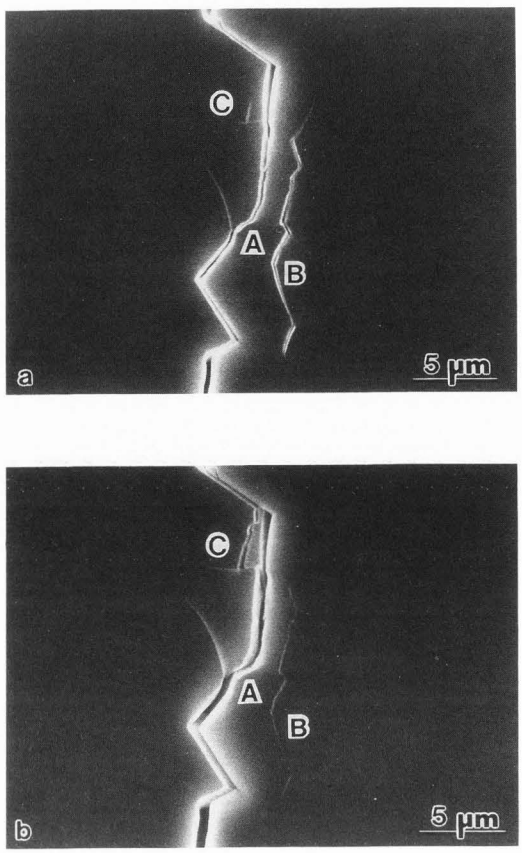

Figure 3. SEM micrographs of region showing closure force at A and secondary cracks at B and C; a) 330 μm behind the crack tip and b) after further loading the crack grows and the region is now 660 μm behind the crack tip.

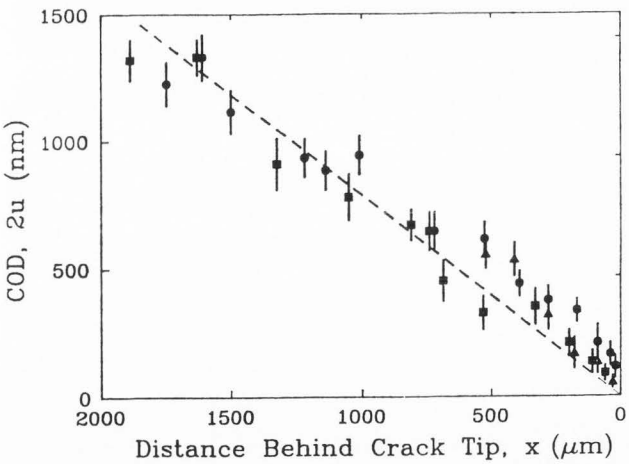

Figure 4. Examples of measured crack opening displacements as function of distance from the crack tip. Different symbols designate different runs; dashed line gives empirical linear fit.

case of the alumina studied, complete closure at a residual applied force was found. An example of a microstructural element bridging the crack faces of an equilibrated crack and a closed crack (in this case, no applied loading) is given in Fig. 5 a,b. The crack in Fig. 5b is virtually invisible and can only be visualized by following the trace of grains released from their original positions.

The case study on alumina thus demonstrates the use of the loading stage and the ability to gain valuable qualitative and quantitative information on the micromechanics operative in the crack wake and, possibly, at the crack tip. The experimental observations focus on the occurrence of microcracks or grain bridging (in other cases this might be fiber, whisker or ductile ligament bridging). Quantitative measurements focus on the crack opening displacement as a function of either applied load or distance from the crack tip.

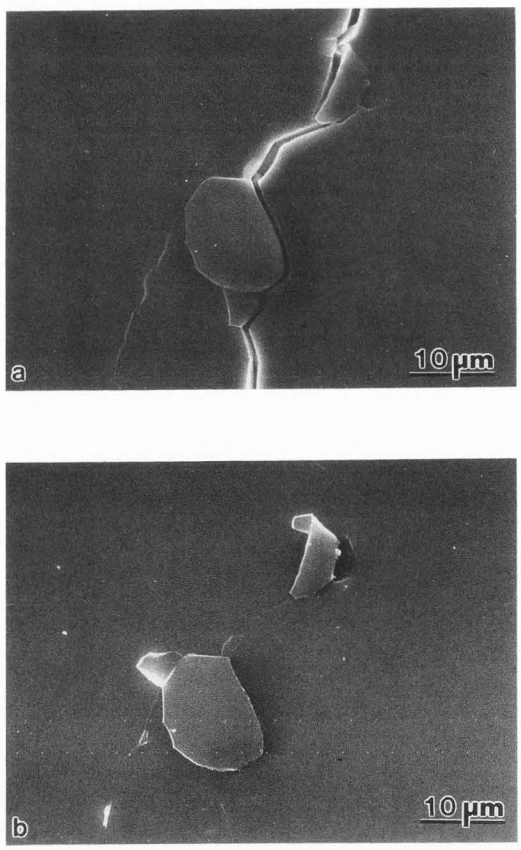

Figure 5. SEM micrographs of areas 1000 μm behind the crack tip showing grain release from the specimen surface; a) maximum applied load corresponding to crack equilibrium, b) zero applied load.

Future Opportunities

The loading device in its current developmental stage is well suited for in situ studies of toughening mechanisms such as grain bridging, ductile ligament or whisker toughening as well as microcrack toughening.

Future advancements are sought in the areas of specimen geometry, and mode of applied loading.

In order to use K-field solutions for the standard geometries (ASTM), it is necessary to propagate a crack through a constant-thickness region. The preliminary aid of a quasi-chevron geometry should therefore be eliminated.

In situ observations during cyclic fatigue are currently under way. The evolution of bridges after given numbers of cycles can be monitored. The closure forces in the crack wake after cyclic loading can also be obtained by evaluating the crack opening displacements.

Further modifications of the fracture device are envisioned to provide the capability of compressive loading and therefore, also compression - compression fatigue. This would then allow inclusion of 4 - pt. bend fixtures as an additional option. A separate biaxial flexure stage is currently under construction. This new device will make it possible to test indentation cracks and will thus give an opportunity to investigate short vs. long crack behavior in the SEM.

Summary

A fracture device which allows in situ observations of crack propagation in brittle solids under tensile loading has been described. It affords the opportunity to study the micromechanics of microstructural elements, which, acting as an ensemble, effect an increase in toughness over samples without special toughening features. The ability to measure applied load, crack opening and crack length makes the loading stage more than an in situ device for qualitative observations, but allows its use as a universal fracture testing machine. Quantitative measurements of the crack opening displacement allow evaluation of the closure stresses acting in the crack wake and enable a further characterization of the closure stress. Future opportunities include cyclic fatigue testing, compressive loading and biaxial flexure.

Acknowledgements

We are indebted to Brian R. Lawn for suggesting this project and continued discussions. We also wish to thank Michael A. Hall for his excellent machining work. Funding was provided by the U.S. Air Force Office of Scientific Research.

References

[1] American Society for Testing and Materials. (1989). E-399-83. pp. 506-508. A.S.T.M. Philadelphia.

[2] Atkins AM, Mai Y-W. (1985). Elastic and plastic fracture. pp. 198-219. Ellis Harwood Limited.

[3] Barenblatt GI. (1962). The mathematical theory of equilibrium cracks in brittle fracture. Adv. Appl. Mech. 7 55-129.

[4] Bennison SJ, Lawn BR. (1989). Role of interfacial grain-bridging sliding friction in the crack-resistance and strength properties of nontransforming ceramics. Acta metall. 37 [10] 2659-2671.

[5] Davidson DL, Nagy A. (1978). A low-frequency cyclic-loading stage for the SEM. J. Phys. E: Sci. Instrum. 11, 207-210.

[6] Evans AG. (1990). Perspective on the development of high-toughness ceramics. J. Am. Ceram. Soc. 73 [2] 187-206.

[7] Evans AG, Faber KT. (1984). Crack-growth resistance of microcracking brittle materials. J. Am. Ceram. Soc. 67 [4] 255-260.

[8] Frei H, Grathwohl G. (1989). Development of a piezotranslator-based bending device for in situ SEM investigations on high-performance ceramics. J. Phys. E: Sci. Instrum. 22, 589-593.

[9] Hübner H, Jillek W. (1977). Sub-critical crack extension and crack resistance in polycrystalline alumina. J. Mat. Sci. 12, 117-125.

[10] Irwin GRI. (1958). Fracture. Handbuch der Physik. 6,551-590.

[11] Knehans R, Steinbrech R. Memory effect of crack resistance during slow crack growth in notched Al_2O_3 bend specimens. J. Mat. Sci. Lett. 1,327-329.

[12] Rice RW. (1988). Perspective on fractography. In: Fractography of glasses and ceramics, Varner JR, Frechette VD, Eds. pp. 3-53.

[13] Rice RW, Freiman SW. (1981). Grain-Size Dependence of Fracture Energy in Ceramics: II, A Model for Noncubic Materials. J. Am. Ceram. Soc. 64 [6] 350-354.

[14] Rödel J, Kelly JF, Lawn BR. (1990). In situ measurements of crack interfaces in the SEM. J. Am. Ceram. Soc. in press.

[15] Swanson PL. (1988). Crack-interface traction: A fracture-resistance mechanism in brittle polycrystals. In: Fractography of glasses and ceramics. Varner JR, Frechette VD. Eds. pp. 135-155.

[16] Swanson PL, Fairbanks CJ, Lawn BR, Mai Y-W, Hockey BJ. (1987). Crack-interface grain bridging as a fracture resistance mechanism in ceramics: I, Experimental Study on Alumina. J. Am. Ceram. Soc. 70 [4] 279-288.

[17] Tait RB, Garrett GG. (1986). Direct observation of fracture in brittle materials in the SEM using a double torsion testing technique. Scanning 8,129-138.

[18] Wiederhorn SM, Johnson H, Diness AM, Heuer AH. (1974). Fracture of glass in vacuum. J. Am. Ceram. Soc. 57 [8] 336-341.

[19] Wu CC, Rice RW, Becher PF. (1981). The character of cracks in fracture toughness measurements of ceramics. In: Fracture mechanics methods for ceramics, rocks and concrete, ASTM STP 745, Freiman SW, Fuller ER. Eds. pp. 127-140.

Discussion with Reviewers

D.L. Davidson: If material is (virtually) elastic why doesn't COD vary with the square root of the distance behind tip (rather than distance behind the tip)? Crack bridging would be more convincing if a variation in COD were illustrated (Why not a graph of COD from Fig. 3?). This may be done in [14] but that's not accessible.

Authors: Elastic simply means non-permanent deformation. A parabolic profile describes cracks with stress-free crack walls, a non-parabolic profile points to forces applied at the crack walls, not necessarily affecting the elastic behavior of the material. Crack openings can only be meaningfully measured where no secondary cracking occurs. The resolution of our method is also not good enough to measure the effect of just one bridge, which might affect the crack opening by only a few nanometers. The closure stresses, however, are far reaching and, taken cumulatively, can be evaluated using a profile measurement [14]. Alternatively, the opening of a secondary crack at a bridge site can also give information about the closure stress [14].

H. Mueller: Can the crack jumping or slipping process be related to microstructure? Is it likely that the advancing crack was inhibited at grain boundaries or is it likely that the grain interiors contained inhomogeneities (even though appearing homogeneous) to account for the crack stick-slip behavior? Can the molecular configuration of the alumina account for this behavior?

Authors: Discontinuous crack advancement is related to variabilities in the microstructure, like variability in the local stresses, the grain boundary toughness, etc.

H. Mueller: Mention is made for obtaining quantitative information by recording COD during loading/reloading. This is essentially the procedure used for determining fracture toughness via chevron-notched methodology which is now well established. With the loading device described herein, it does seem possible to record load vs COD thereby providing a means to determine a plane strain fracture toughness. Has any consideration been given to relating the load vs COD plots to microstructure via SEM analysis. With this in mind, the chevron-notch geometry can therefore be beneficial instead of what is stated as preliminary and intended for elimination.

Authors: The methodology mentioned does not lend itself easily to measurement of R-curve behavior. Detailed mathematical calulations of the relevant R-curves from the crack profile for this material can be found in [14].

H. Mueller: The presence of residual stresses can be compressive and tensile in nature. Mention is made of crack closure stresses which are likely due to compressive residual stresses. In the case of residual tensile stresses, can it be thought that crack opening stresses may instead be generated along the crack? If this is so, crack weakening instead of crack toughening would be operative.

Authors: The residual compressive and tensile stresses perpendicular to the crack plane indeed average out to zero. The residual stresses related to bridge formation (enhanced secondary cracking, clamping of grains etc.) allow for the generation of closure stresses.

H. Mueller: Was an angle of 28° critical for obtaining crack propagation stability? If a chevron angle of about 9 1/2° was used instead and extended to about 6 mm on the unpolished disc surface, their would have been no need to remove the samples to resaw after a crack was grown to 2 mm. If 28° was optimal, a thicker sample size of about 3 mm could also have been used to grow cracks to 6 mm in length within the quasi chevron-notched region without stopping to remove and resaw the samples.

Authors: The angle of 28° was rather arbitrarily chosen. Since the area of bridged crack walls has to be kept identical from experiment to experiment, the identical chevron geometry has to be used and the suggestion is not applicable.

H. Mueller: The COD vs distance from the crack tip plot shown in Figure 4 is apparently without crack bridging mechanisms being included. If crack bridging is included within regions along the crack, how would a typical COD vs distance plot be characterized? One might think that a parabolic profile or some other decreasing profile would be depicted in this situation and that a linear profile would be depicted with a stress-free surface (just the opposite of that mentioned).

Authors: From standard fracture mechanics theory we know [3,10]: Stress-free crack surfaces lead to a parabolic profile. Figure 4 includes crack bridging (not parabolic).